Blood flow dynamics in the total cavopulmonary connection long-term after Fontan completion

Rijnberg, F.M.

CHAPTER 7B

Extracardiac conduit adequacy along the respiratory cycle in adolescent Fontan patients

Friso Rijnberg, Séline van der Woude, Mark Hazekamp, Pieter van den Boogaard, Hildo Lamb, Covadonga Terol Espinosa de Los Monteros, Lucia Kroft, Sasa Kenjeres, Tawab Karim, Monique Jongbloed, Jos Westenberg, Jolanda Wentzel, Arno Roest

European Journal of Cardiothoracic Surgery 2021

Abstract

Background

Adequacy of 16-20mm extracardiac conduits for adolescent Fontan patients remains unknown. This study aims to evaluate conduit adequacy using the inferior vena cava (IVC)-conduit velocity mismatch factor along the respiratory cycle.

Methods

Real-time 2D flow MRI was prospectively acquired in 50 extracardiac (16-20mm conduits) Fontan patients (mean age 16.9±4.5 years) at the subhepatic IVC, conduit and superior vena cava. Hepatic venous (HV) flow was determined by subtracting IVC flow from conduit flow. The cross-sectional area (CSA) was reported for each vessel. Mean flow and velocity was calculated during the average respiratory cycle, inspiration and expiration. The IVC-conduit velocity mismatch factor was determined as follows: $V_{conduit}/V_{IVC}$, where V is the mean velocity.

Results

Median conduit CSA and IVC CSA were 221mm^2 (Q1-Q3 201-255) and 244mm^2 (Q1-Q3 203-265), respectively. From the IVC towards the conduit, flow rates increased significantly due to entry of HV flow (IVC 1.9, Q1-Q3 1.5-2.2) vs conduit (3.3, Q1-Q3 2.5-4.0 L/min, $p<0.001$). Consequently, mean velocity significantly increased (IVC 12 (Q1-Q3 11-14 cm/s) vs conduit 25 (Q1-Q3 17-31cm/s), $p<0.001$), resulting in a median IVC-conduit velocity mismatch of 1.8 (Q1-Q3 1.5-2.4), further augmenting during inspiration (median 2.3, Q1-Q3 1.8-3.0). IVC-conduit mismatch was inversely related to measured conduit size and positively correlated with conduit flow. A weak inverse correlation was present between the expiratory normalized mismatch factor and peak VO2 ($r=0.37$, $p=0.014$).

Conclusion

Important blood flow accelerations are observed from the IVC towards the conduit in adolescent Fontan patients which is related to peak V02. This study therefore raises concerns that implanted 16-20mm conduits have become undersized for older Fontan patients and future studies should clarify its effect on long-term outcome.

Introduction

The Fontan procedure provides a palliative solution for single ventricle patients, by connecting both the superior (SVC) and inferior vena cava (IVC) directly to the pulmonary arteries (i.e. Total CavoPulmonary Connection, TCPC). Nowadays, most centers complete the TCPC by connecting the IVC to the right PA using a Goretex extracardiac conduit at an age of 2-4 years[1]. However, the lack of growth potential remains concerning for older Fontan patients. To date, optimal conduit size for adult Fontan patients is unknown as no clear definition is available to describe the hemodynamic adequacy of extracardiac conduits during follow-up, beyond identifying a distinct stenosis within the Fontan conduit.

The extracardiac conduit directs 65-70% of total systemic venous return towards the PAs[2]. Since blood flow resistance is inversely related to the fourth power of the vessel radius (law of Hagen-Poiseuille), an undersized conduit leads to reduced TCPC flow efficiency[3-5] Exercise performance has been associated with conduit size[6, 7], which is related to TCPC flow efficiency[3, 8]. On top of that, TCPC flow efficiency has been associated with the degree of liver fibrosis, a common complication in Fontan palliated patients[9].

Recently, the *IVC-conduit velocity mismatch factor* has been proposed as a marker of conduit adequacy, describing the change in mean velocity from the subhepatic IVC towards the conduit[10]. In that study, 4D flow MRI revealed important blood flow acceleration at the level of the conduit that were associated with increased viscous energy losses resulting in less efficient TCPC blood flow.[10] Since conduit flow changes along the respiratory cycle due to intrathoracic pressure changes, evaluation of the IVC-conduit velocity mismatch along the respiratory cycle may reveal important insights in the adequacy of the conduit size during both inspiration (highest flow) and expiration (lowest flow).

The hypothesis is that adolescent Fontan patients may outgrow implanted conduit size, leading to an increased blood flow velocity from the subhepatic IVC towards the conduit. Therefore, the aim is to assess conduit adequacy along the respiratory cycle by evaluating the IVC-conduit velocity mismatch factor using real-time 2D flow MRI and determine its relationship with exercise performance.

Material and Methods

Study population

Fontan patients with an extracardiac Goretex conduit prospectively underwent MRI between 2018-2020 at the Leiden University Medical Center, Leiden, the Netherlands. All patients >8 years old without contraindications for MRI were eligible for inclusion. The study was approved by the medical ethical review board of the hospital. Written informed consent was obtained from all patients and/or their parents.

Magnetic resonance imaging

MRI acquisition details are presented in Supplemental Table 1. Real-time 2D phase contrast MRI measurements were obtained at the level of the subhepatic IVC (below entry of the HVs), the extracardiac conduit and the SVC (Figure 1A). HV flow was indirectly determined by subtracting IVC flow from conduit flow. Measurements consisted of 250 real-time (non ECG-gated) flow acquisitions with a sample rate of approximately 15 frames per second. The respiratory signal was continuously monitored using an air-filled abdominal belt. Flow rate (Q), mean velocity (V) and cross-sectional area (CSA) of each vessel was acquired by manual segmentation of the vessel lumen on all phase-contrast images (Figure 1B, Mass software, Leiden, the Netherlands). The mean CSA during the entire flow acquisition is reported.

The workflow of the real-time 2D flow MRI analysis is shown in Figure 1 and Supplemental material 1. Typically, 2-4 consecutive respiratory cycles and associated flow and velocity curves were automatically cut into inspiration and expiration phases using in-house developed software (Figure 1C). A single flow curve was derived (Figure 1D-F) from the average inspiratory and expiratory flow curves, which was used for the analysis of the flow parameters. To determine real-time HV flow, inspiratory and expiratory flow curves from the IVC and conduit were aligned and subsequently subtracted.

Mean flowrates and velocities (V) were determined during the entire respiratory cycle, inspiration and expiration. The ratio between mean inspiratory and mean expiratory flowrates was calculated as a marker of respiration-driven pulsatility (Q_{insp}/Q_{exp}). Retrograde flow fraction was calculated by dividing retrograde flow volume (retrograde flow rate * duration of retrograde flow) by antegrade flow volume.

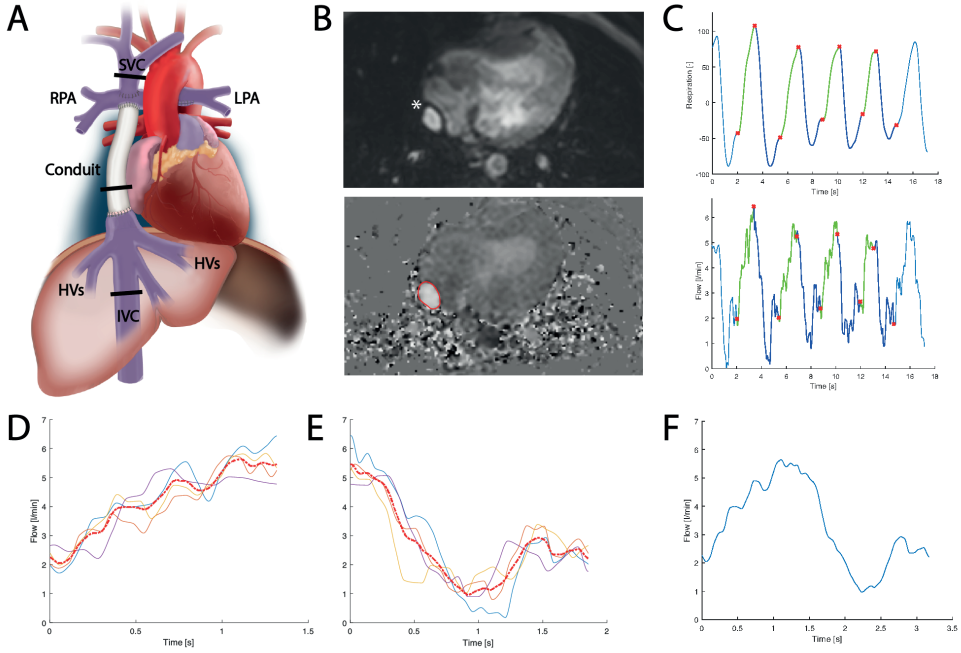

Figure 1. Figure 1 shows the workflow of the real-time 2D flow MRI analysis of a conduit flow measurement. The same analysis is applied to the subhepatic IVC and SVC. The position of the 2D flow planes are shown (A). The lumen of the conduit (*) was manually delineated on the phase contrast images. Multiple consecutive respiratory curves and corresponding flow curves (C) were automatically divided into multiple inspiration (green) and expiration (blue) parts. After interpolation, a single average curve was generated from the individual inspiratory (D) and expiratory (E) curves and subsequently combined to acquire the average respiratory cycle (F).

IVC-conduit velocity mismatch factor

The IVC-conduit velocity mismatch factor was determined for the average respiratory cycle, inspiration and expiration phases as follows: $V_{conduit}/V_{IVC}$, where V is the mean velocity in the conduit and subhepatic IVC, respectively. A mismatch factor of 1 represents equal mean velocity (ideal), <1 represent a decrease in mean velocity (oversized conduit) and >1 represents an increase in mean velocity (undersized conduit).

The relation between the IVC-conduit velocity mismatch factor and mean conduit flow rates was analyzed by grouping patients in tertiles of measured conduit CSA: <209mm^2 (n=16), 209-241mm^2 (n=17) and >241mm^2 (n=17). Grouping patients on measured conduit size rather than on implanted conduit size is based on observations that conduit CSA can variably decrease after implantation due to neointima formation and conduit stretching[7, 11, 12]. To put CSA values in perspective to implanted conduit diameters, the theoretical CSA corresponding to 16-20mm circular conduits is 201mm^2

(16mm), 254mm^2 (18mm) and 314mm^2 (20mm). Furthermore, vessel CSA normalized for the average flow rate during the respiratory cycle in each vessel is presented. To compare IVC-conduit velocity mismatch between measured conduit size groups, values were normalized for indexed conduit flow rate (L/min/m^2).

Cardiopulmonary exercise testing

Cardiopulmonary exercise testing was performed on an upright bicycle ergometer (GE Healthcare, Wisconsin, USA). A continuous incremental bicycle protocol was executed according to the Godfrey protocol. Patients had to maintain a pedaling rate of 60 revolutions/min and were encouraged to cycle to exhaustion. Peak VO2 (ml/kg/min) was determined in all patients with a respiratory exchange ratio >1.0.

Statistical analysis

Data were presented as median (Q1-Q3) or mean (standard deviation). Normal distributions of continuous data were tested using the Shapiro-Wilk test. Correlation analysis was performed using Pearson or Spearman correlation (weak 0.3-0.5, moderate 0.5-0.7, strong ≥0.7-0.9 and very strong >0.9). Measurements between the different vessels were compared using a paired t-test or Wilcoxon signed-rank test. Comparison of normalized mismatch factor between measured conduit size tertiles were performed using the Kruskal-Wallis test (adjusted for multiple comparisons using Bonferroni). A p-value <0.05 was considered statistically significant. Data were analyzed with SPSS 25.0 (IBM Corp., Armonk, NY, USA) and Graphpad Prism 8.0 (GraphPad Software, La Jolla, California, USA).

Results

Fifty-seven extracardiac conduit Fontan patients underwent MRI examination. Seven patients with incomplete 2D real-time MRI examinations were excluded from analysis. Patient characteristics are provided in Table 1. CPET was performed in 47/50 patients, with 44 patients reaching maximal effort (median time between CPET and MRI 0 days (Q1-Q3 0-15 days).

Table 1. Patient characteristics

Male/Female, n	24/26
Primary diagnosis, n(%)	
- TA	12(24)
- HLHS	10(20)
- DILV + TGA	10(20)
- DORV	6(12)
- uAVSD	4(8)
- ccTGA	4(8)
- PA + IVS	2(4)
- Other	2(4)
Dominant ventricle	
Left, n(%)	29(58)
Right, n(%)	16(32)
Biventricular/indeterminate, n(%)	5(10)
Characteristics at Fontan procedure	
Age at Fontan, years	3.7(1.9)
Implanted conduit size (16/18/20mm), n	26/18/6
Height, cm	99(11)
Weight, kg	15.0(2.9)
BSA, m^2	0.64(0.09)
Characteristics at time of MRI	
Age at MRI, years	16.9(4.5)
Height, cm	167(11)
Weight, kg	57(14)
BSA, m^2	1.62(0.24)
Time between Fontan and MRI, years	13.2(4.1)
NYHA-class I-II, n (%)	50(100)
CPET	
Peak VO2 (n=44), ml/kg/min	26.4(5.6)

Values are reported as mean (SD) unless otherwise specified. TA; tricuspid atresia, HLHS; hypoplastic left heart syndrome, DILV; double inlet left ventricle, (cc)TGA; (congenital corrected) transposition of the great arteries, DORV; double outlet right ventricle, uAVSD; unbalanced atrioventricular septal defect, PA+IVS; pulmonary atresia with intact ventricular septum, CPET; cardiopulmonary exercise testing

Cross-sectional area

IVC and conduit CSA were a median of 244mm^2 (Q1-Q3 203-265) and 221mm^2 (Q1-Q3 201-255), respectively. CSA decreased from the subhepatic IVC towards the conduit with a median of 9% (Q1-Q3 -18-15), with IVC CSA exceeding conduit CSA in 30 patients (60%). Median normalized conduit CSA (66mm^2 per L/min, Q1-Q3 54-97) was smaller compared to normalized IVC CSA (129mm^2 per L/min, Q1-Q3 118-148, $p<0.001$), decreasing a median of 44% (Q1-Q3 33-58% decrease).

Measured conduit CSA of implanted 16-20mm conduits were 101% (Q1-Q3 93-109%), 97% (Q1-Q3 88-108%) and 94% (Q1-Q3 70-96%) of theoretical expected conduit CSA, respectively. Of note, measured conduit CSA exceeded the theoretically expected conduit CSA in some patients which can be explained by methodological reasons (see limitation section). In 2/6 patients with a 20mm conduit, measured conduit CSA was 232mm^2 and 192mm^2, 27% and 39% decreased compared to expected theoretical conduit CSA. The median measured conduit CSA after subdividing the patients in tertiles were per group 191mm^2 (Q1-Q3 172-201), 220mm^2 (Q1-Q3 214-228) and 277mm^2 (Q1-Q3 251-302), respectively.

Flow

Along the entire respiratory cycle, flow rates increased from the IVC (median 1.9, Q1-Q3 1.5-2.2 L/min) towards the conduit (median 3.3, Q1-Q3 2.5-4.0 L/min, $p<0.001$, Table 2) because of entry of HV flow (median increase 77% (Q1-Q3 59-104%)). HV flow was strongly dependent on respiration, with a median Q_{insp}/Q_{exp} ratio of 3.0 (Q1-Q3 2.2-4.1). During inspiration, expiration and the entire respiratory cycle, respectively, 57% (Q1-Q3 50-60), 30% (Q1-Q3 21-39) and 43% (Q1-Q3 37-51) of total conduit flow originated from the HVs.

The median Q_{insp}/Q_{exp} ratio was 1.2 (Q1-Q3 1.1-1.4) in the SVC, 1.1 (Q1-Q3 1.0-1.3) in the IVC and 1.7 (Q1-Q3 1.5-2.1) in the conduit. Therefore, most pulsatility observed in the conduit originates from the pulsatile HV flow. Retrograde flow was negligible at the level of the conduit, SVC and IVC in all patients, but occurred in the HVs in 43 (86%) patients, exclusively in (early) expiration.

IVC-conduit velocity mismatch

Mean velocities in the IVC and SVC were generally low (range 10-14cm/s) during all respiratory phases (Table 2). The combination of a decrease in CSA and an increase in flow rate resulted in higher mean velocity in the conduit compared to the IVC ($p<0.001$ for all respiratory phases). The median IVC-conduit velocity mismatch factor during the entire respiratory cycle was 1.8 (Q1-Q3 1.5-2.4), indicating a 1.8 fold increase of the mean velocity from the subhepatic IVC towards the conduit.

Table 2. Subhepatic IVC, HV, conduit and SVC characteristics

Cross-sectional area (mm^2)	**Absolute CSA (mm^2)**	**Normalized CSA (mm^2 per L/min)**		
IVC	244(203-265)	129(118-148)		
Conduit	221(201-255)	66(54-97)		
SVC	218(161-256)	150(129-197)		
Change in CSA from IVC to conduit,%	-9(-18-15)	-44(-58- -33)		
Flow(L/min)	**Entire respiratory cycle**	**Inspiration**	**Expiration**	**Q_{insp}/Q_{exp} ratio**
IVC	1.9(1.5-2.2)†,‡	2.1(1.6-2.5)‡,§	1.7(1.3-2.1)†,§	1.1(1.0-1.3)
HV	1.5(1.0-1.8)†,‡	2.6(2.1-3.1)‡,§	0.7(0.5-1.2)†,§	3.0*(2.2-4.1)
Conduit	3.3(2.5-4.0)†,‡	4.5(3.9-5.3)‡,§	2.6(1.9-3.3)†,§	1.7(1.5-2.1)
SVC	1.3(1.1-1.6)†,‡	1.5(1.3-1.8)‡,§	1.2(1.0-1.5)†,§	1.2(1.1-1.4)
Change in flow from IVC to conduit,%	77(59-104)†,‡	131(99-152)‡,§	44(27-65)†,§	
Contribution of HV flow to conduit flow,%	43(37-51)†,‡	57(50-60)‡,§	30(21-39)†,§	
Retrograde-to-antegrade flow ratio IVC,%	0(0-0)	0(0-0)	0(0-0)	
Retrograde-to-antegrade flow ratio HV,%	5(1-9)†,‡	0(0-0)‡,§	13(3-31)†,§	
Retrograde-to-antegrade flow ratio Conduit,%	0(0-0)	0(0-0)	0(0-0)	
Retrograde-to-antegrade flow ratio SVC,%	0(0-0)	0(0-0)	0(0-0)	
Mean velocity(cm/s)	**Entire respiratory cycle**	**Inspiration**	**Expiration**	
IVC	12(11-14)†,‡	13(12-16)‡,§	12(10-14)†,§	
Conduit	25(17-31)†,‡	35(25-40)‡,§	19(12-25)†,§	
SVC	11(9-13)†,‡	13(10-15)‡,§	10(8-12)†,§	
IVC-conduit velocity mismatch factor	1.8(1.5-2.4)†,‡	2.3(1.8-3.0)‡,§	1.5(1.2-2.1)†,§	

Values are reported as median (Q1-Q3). IVC/SVC; inferior/superior vena cava, HV; hepatic venous, CSA; cross-sectional area, L/min, liter per minute, cm/s, centimeter per second. *3 cases with negative ratios were excluded. P-value <0.001 compared to inspiration†, expiration‡ or the entire respiratory cycle§.

Because of the important respiratory dependency of HV flow, IVC-conduit velocity mismatch was higher during inspiration (median 2.3, Q1-Q3 1.8-3.0), P<0.001) and lower during expiration (median 1.6, Q1-Q3 1.2-2.1, P<0.001, Figure 2, Supplemental Video 1) compared to the entire respiratory cycle. A moderate positive correlation was found between mean conduit flow rate and the IVC-conduit velocity mismatch factor during the entire respiratory cycle (r=0.58), inspiration (r=0.42) and expiration (r=0.69, Figure 3). Highest mismatch was present in the group with smallest conduits (Group 1 <209mm^2, Figure 3&4). Up to a 4.4-fold increase in mean velocity was observed during inspiration in Group 1 patients with high flow rates (Figure 3B). Importantly, only 5 patients (10%) had a mismatch factor <1 during expiration indicating flow expansion due to an relatively oversized conduit (all in Group 2-3, age 10-14 years, Figure 3B).

The normalized IVC-conduit velocity mismatch factor during expiration and the entire respiratory cycle correlated with peak VO2 (r= -0.37, p=0.014 and r= -0.31, p=0.04, respectively).

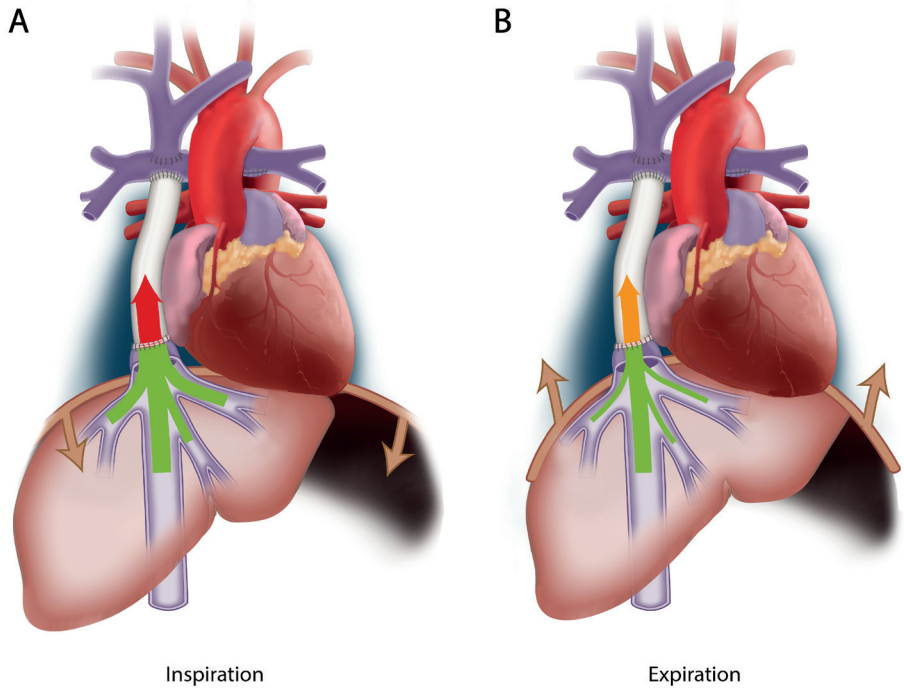

Figure 2. The presence of IVC-conduit velocity mismatch is schematically shown during inspiration **(A)** and expiration **(B)**. The thickness of the arrow indicates the amount of flow and the color indicates the blood flow velocity. An important increase in mean velocity is observed from the subhepatic IVC towards the conduit in both inspiration (highest mismatch) and expiration.

A moderate positive correlation was found between BSA and mean conduit flow during all respiratory phases (r= 0.62-0.70), with considerable variation in flow rates between patients with similar body sizes (Supplemental Figure 1). No correlation was found between IVC mean velocity and BSA (r=0.26, p=0.06).

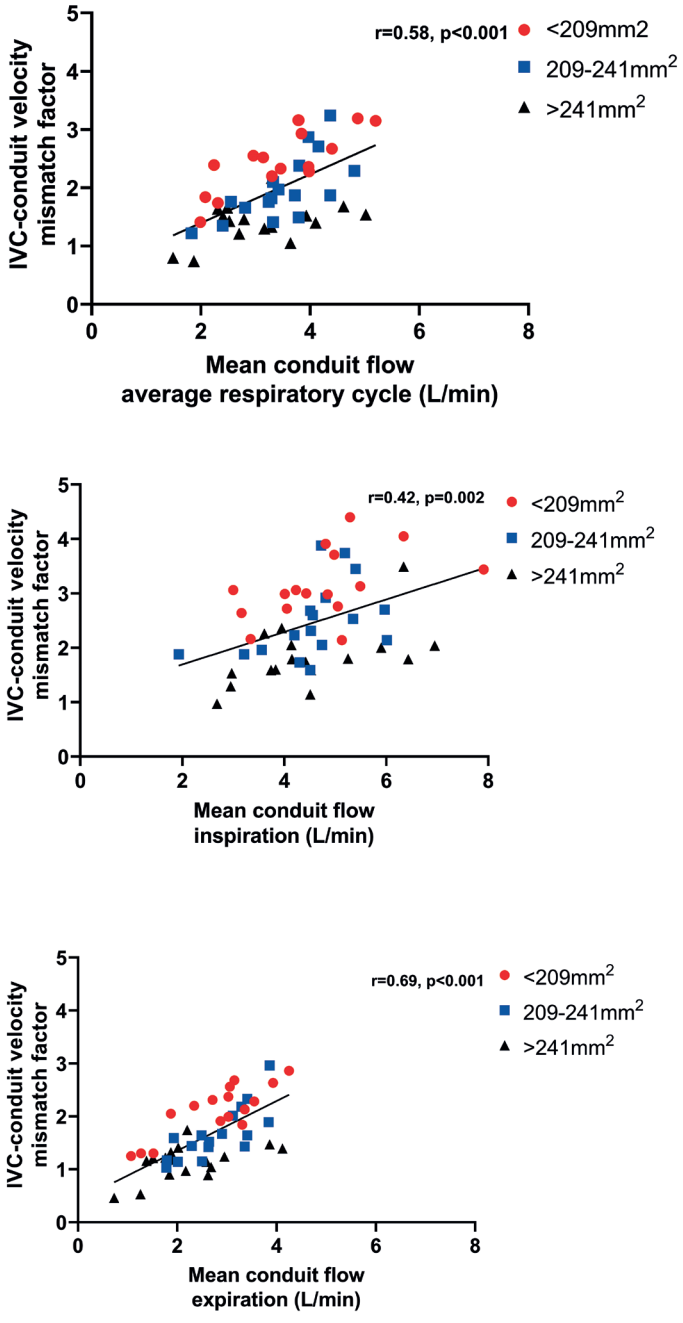

Figure 3. The correlation between conduit flow rate and IVC-conduit velocity mismatch factor is shown for the entire respiratory cycle (A), inspiration (B) and expiration (C). Patients are color-coded into three groups based on the measured conduit size for visualization purposes only.

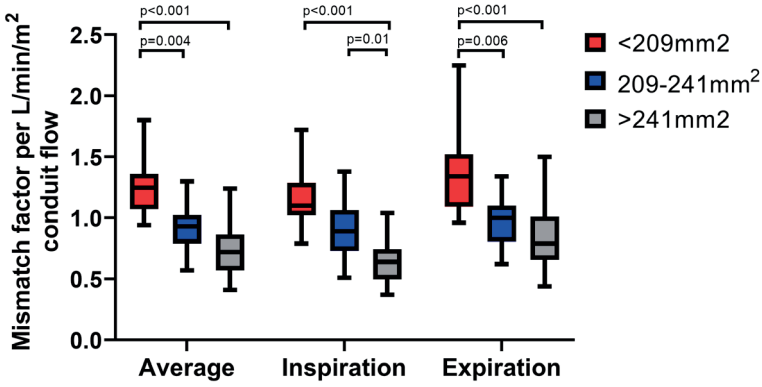

Figure 4. The IVC-conduit velocity mismatch factor normalized for conduit flow rate per BSA is shown for the average respiratory cycle, inspiration and expiration for the 3 groups of measured conduit size. E.g., a normalized IVC-conduit mismatch factor of 0.5 means an increase in velocity from the IVC towards the conduit when conduit flow rate is >2 L/min/m^2.

Discussion

This study evaluated the hemodynamic adequacy of implanted 16-20mm extracardiac conduit sizes along the respiratory cycle at a mean interval of 13 years after Fontan completion. The main findings show that at a mean age of 17 years, absolute conduit CSA is 9% smaller as compared to the CSA of the subhepatic IVC, even though all HV flow still needs to enter the IVC. Consequently, important blood flow accelerations (IVC-conduit velocity mismatch) are present from the subhepatic IVC towards the conduit which are further augmented during inspiration. The normalized IVC-conduit mismatch factor during expiration and the entire respiratory cycle inversely correlated with peak VO2. This study raises concerns that implanted 16-20mm conduits have become undersized for adolescent Fontan patients.

Currently, typically 16-20mm conduits are implanted in a 'one size fits all approach', with all children receiving approximately the same conduit size despite different projected adult body size and related flow conditions. Itatani et al. recommended 16-18mm conduits for 2-3 year old patients based on evaluation of energy loss and flow stagnation using computational fluid dynamics in young Fontan patients (mean BSA 0.5, 3.0 years old, mean conduit flow 0.85 L/min). Conduit size recommendations for older Fontan patients could therefore not be determined. In comparison, in our study BSA and conduit flow rates were approximately 3-4 times higher. In a recent expert review, implantation of 16-18mm conduits are recommended, with larger conduit sizes being associated with worse exercise capacity.[6, 13] However, late studies evaluating

hemodynamics of these conduit sizes in older Fontan patients are currently lacking. The proposed adequacy of 16-20mm conduit sizes for adult Fontan patients has also been based on IVC diameters in healthy adults[12, 14]. Interestingly, the subhepatic IVC diameter is already in the order of 18mm in healthy adults.[15] The mean suprahepatic IVC diameter, distal to entry of the HVs, is significantly larger to account for the increase in flow rate caused by the HVs; a mean of 24mm (CSA 452mm^2) in healthy adults[16], 27mm (CSA 572mm^2) in adults with congenital heart disease[16] up to even 770mm^2 in adult Fontan patients[17]. In our study, median conduit CSA was only 221mm^2 and a median 9% smaller compared to the **sub**hepatic IVC CSA, indicating that implanted conduits have become undersized. This is a result of both somatic growth leading to increased flow rates and CSA of surrounding vessels, but also by a decrease in actual conduit CSA during follow-up due to stretching/neo-intima formation in some patients. [7, 11, 12] Congestion most likely did not play a role in the size of the IVC, as no negative correlation was found between BSA and IVC mean velocity.

Previously, our group published the concept of IVC-conduit velocity mismatch based on observations using 4D flow MRI[10]. This parameter is based on the concept that both flow expansion (decrease in velocity) and flow contraction (increase in velocity) should ideally be absent to avoid increased energy loss and/or thrombosis risk.[18] Indeed, mean velocities remained in a relatively narrow range in the native subhepatic IVC and SVC, indicating that these vessels adapt to change in flow rates over time. The rigid extracardiac conduits lacks this physiologic adaptation, explaining the increase in mean conduit velocity with higher conduit flow rates. This becomes evident when looking at the vessels CSA normalized for flow, which was a median 44% smaller for the conduit compared to the IVC. Importantly, IVC-conduit velocity mismatch >1 was already present during expiration in 90% of patients, furthermore indicating that these conduits have become relatively undersized even during the respiratory phase with lowest flow rates.

In light of the reported normal suprahepatic IVC diameters in healthy adults, it is not surprising that we observed a median mismatch factor of 1.8, as median conduit size was only 221mm^2. Since Q=V*A (where Q is the flow rate, V is the mean velocity and A is the cross-sectional area), conduit CSA must theoretically be a 1.8-fold higher in our cohort to avoid an increase in mean velocity, effectively indicating a long-segmental stenosis of approximately 50%. These projected values would be in line with suprahepatic CSA observed in healthy persons[16]. Interestingly, the CSA of an intra-atrial lateral Fontan tunnel, in which part of the tunnel wall consists of atrial tissue with growth potential, is already 420-580mm^2 (23-27mm) at an age of 10-15 years.[19, 20] Thus, the physiologic response to increased flow rates during somatic growth seems to lead to importantly larger intra-atrial Fontan tunnels compared to the rigid extracardiac conduit.

Clinical relevance: TCPC efficiency and long-term outcome

The observed IVC-conduit velocity mismatch may be of clinical relevance, as the conduit plays an important role in TCPC hemodynamics. Efficient and unobstructed TCPC blood flow with minimal energy loss is desired to minimize the elevation in CVP while ensuring optimal preload in Fontan patients.[5, 21] On average, 65-70% of total systemic venous return enters the TCPC via the conduit, further increasing to 79% during lower-leg exercise[2]. Since blood flow resistance is inversely proportional to the fourth power of the vessel radius (law of Hagen-Poiseuille), undersized conduits are among the most important factors of TCPC resistance.[3] In a large study of CFD simulations during resting conditions, patients with small Fontan conduits showed a 3-fold higher TCPC resistance compared to the mean resistance of the entire study cohort, potentially reaching values up to 35-50% of normal pulmonary vascular resistance.[5] TCPC resistance further increases exponentially during exercise[22] while pulmonary vascular resistance decreases during exercise[23], making TCPCs with a relatively undersized conduit a potential bottleneck in the Fontan circulation.[4, 24]

Decreased TCPC flow efficiency is associated with reduced preload and thereby cardiac output, associated with a decreased exercise capacity.[5, 21, 25] Our study showed a weak inverse correlation between the normalized IVC-conduit velocity mismatch factor and peak VO2, which might be explained by the increased TCPC resistance in patients with smaller conduits with higher mismatch. This in line with recent findings by Patel et al, who found a correlation between minimum conduit size and predicted peak VO2.[7]

The increased resistance caused by undersized conduits will lead to an elevated central venous pressure (CVP) to maintain cardiac output, which plays an important role in the pathophysiology of protein losing enteropathy and liver cirrhosis. Fontan patients with an extracardiac conduit show a faster progression of liver fibrosis compared to intra-atrial tunnel Fontan patients.[26] We speculate that the presence of undersized conduits showing important IVC-conduit velocity mismatch might be one of the reasons by increasing afterload for HV flow, especially during inspiration. The acceleration of blood flow in the conduit may also have adverse effects on downstream energy-consuming flow patterns (e.g. vortices, helices) or caval flow collision within the Fontan confluence, further decreasing TCPC flow efficiency.[24]

Potential implications for surgical strategy

Our current practice is to implant 18mm fenestrated conduits in our patients and since long we have abandoned implanting 16mm conduits. However, this study shows that a strategy of implanting rigid conduits in children aged 2-4 years results in suboptimal hemodynamics at older age and is therefore not ideal. As implantation of larger conduit sizes in young children is unfeasible by anatomical constraints as well as undesirable

as they will cause sluggish flow increasing thrombosis risk[14, 18], we believe that conduits of other materials should be considered rather than implanting larger conduits. Currently, stretchable ePTFE grafts (PECALabs) are available which could potentially minimize the decrease in conduit CSA caused by stretching during somatic growth and can be dilated to some extent when the child becomes older. Furthermore, tissue-engineered conduits are being developed and may be promising by allowing for growth.[27]

Based on the current study, it is impossible to speculate which levels of IVC-conduit velocity mismatch warrants replacement of the conduit. It will be important to know how observed IVC-conduit velocity mismatch relates to hemodynamic markers such as pressure drop and resistance and how the mismatch develops over time, which will be essential information for clinical decision making about possible intervention. Essentially any pressure drop from the caval veins towards the PAs is undesirable and pressure gradients as low as ±1mmHg already may form an indication to intervene, although exact cut-off points are not available at this moment. Furthermore, although our cohort represented relatively asymptomatic patients without signs of Fontan failure, the chronic negative effects of IVC-conduit velocity mismatch may only become apparent later in life. Serial studies with comprehensive MRI flow evaluation and longer follow-up are needed to determine the effect of undersized conduits on long-term outcome.

Limitations

Flow rates were analyzed along the respiratory cycle only, irrespective of the phase of the cardiac cycle. Since flow pulsatility along the cardiac cycle is only minimal[28] and predominantly is determined by the respiratory cycle[29], inaccuracies are likely small. Furthermore, CSA was measured from 2D real-time PC-MRI which has a limited spatial resolution and can overestimate CSA when the flow acquisition is not planned precisely perpendicular to the vessel lumen. However, these errors are likely systematic as CSA of all vessels were measured using the same method. HV flow was only measured indirectly by subtracting IVC flow from conduit flow, but results are in strong agreement with a previous study that directly measured HV flow using echocardiography.[30]

Conclusion

This study evaluated the hemodynamic adequacy of extracardiac Goretex conduits sized 16-20mms along the respiratory cycle in Fontan patients. Important IVC-conduit velocity mismatch, i.e. an increase in velocity from the subhepatic IVC towards the conduit, is observed at a mean interval of 13 years after Fontan completion. This raises

concerns that implanted 16-20mm conduits have become undersized for older Fontan patients. The normalized IVC-conduit velocity mismatch factor showed an inverse weak correlation with peak V02. Future studies are warranted to clarify the long-term effect of IVC-conduit velocity mismatch on clinical outcome.

References

[1] Rychik J, Atz AM, Celermajer DS, Deal BJ, Gatzoulis MA, Gewillig MH et al. Evaluation and Management of the Child and Adult With Fontan Circulation: A Scientific Statement From the American Heart Association. Circulation 2019.

[2] Hjortdal VE, Emmertsen K, Stenbog E, Frund T, Schmidt MR, Kromann O et al. Effects of exercise and respiration on blood flow in total cavopulmonary connection: a real-time magnetic resonance flow study. Circulation 2003;108:1227-31.

[3] Tang E, Restrepo M, Haggerty CM, Mirabella L, Bethel J, Whitehead KK et al. Geometric characterization of patient-specific total cavopulmonary connections and its relationship to hemodynamics. JACC Cardiovasc Imaging 2014;7:215-24.

[4] Rijnberg FM, Hazekamp MG, Wentzel JJ, de Koning PJH, Westenberg JJM, Jongbloed MRM et al. Energetics of Blood Flow in Cardiovascular Disease: Concept and Clinical Implications of Adverse Energetics in Patients With a Fontan Circulation. Circulation 2018;137:2393-407.

[5] Haggerty CM, Restrepo M, Tang E, de Zelicourt DA, Sundareswaran KS, Mirabella L et al. Fontan hemodynamics from 100 patient-specific cardiac magnetic resonance studies: a computational fluid dynamics analysis. J Thorac Cardiovasc Surg 2014;148:1481-9.

[6] Lee SY, Song MK, Kim GB, Bae EJ, Kim SH, Jang SI et al. Relation Between Exercise Capacity and Extracardiac Conduit Size in Patients with Fontan Circulation. Pediatr Cardiol 2019;40:1584-90.

[7] Patel ND, Friedman C, Herrington C, Wood JC, Cheng AL. Progression in Fontan conduit stenosis and hemodynamic impact during childhood and adolescence. J Thorac Cardiovasc Surg 2020.

[8] Khiabani RH, Whitehead KK, Han D, Restrepo M, Tang E, Bethel J et al. Exercise capacity in single-ventricle patients after Fontan correlates with haemodynamic energy loss in TCPC. Heart 2015;101:139-43.

[9] Trusty PM, Wei ZA, Rychik J, Graham A, Russo PA, Surrey LF et al. Cardiac Magnetic Resonance-Derived Metrics Are Predictive of Liver Fibrosis in Fontan Patients. Ann Thorac Surg 2020;109:1904-11.

[10] Rijnberg FM, Elbaz MSM, Westenberg JJM, Kamphuis VP, Helbing WA, Kroft LJ et al. Four-dimensional flow magnetic resonance imaging-derived blood flow energetics of the inferior vena cava-to-extracardiac conduit junction in Fontan patients. Eur J Cardiothorac Surg 2019;55:1202-10.

[11] Amodeo A, Galletti L, Marianeschi S, Picardo S, Giannico S, Di Renzi P et al. Extracardiac Fontan operation for complex cardiac anomalies: seven years' experience. J Thorac Cardiovasc Surg 1997;114:1020-30; discussion 30-1.

[12] Cho S, Kim WH, Choi ES, Kwak JG, Chang HW, Hyun K et al. Outcomes after extracardiac Fontan procedure with a 16-mm polytetrafluoroethylene conduit. Eur J Cardiothorac Surg 2018;53:269-75.

[13] Daley M, d'Udekem Y. The optimal Fontan operation: Lateral tunnel or extracardiac conduit? J Thorac Cardiovasc Surg 2020.

[14] Alexi-Meskishvili V, Ovroutski S, Ewert P, Dahnert I, Berger F, Lange PE et al. Optimal conduit size for extracardiac Fontan operation. Eur J Cardiothorac Surg 2000;18:690-5.

[15] Moreno FL, Hagan AD, Holmen JR, Pryor TA, Strickland RD, Castle CH. Evaluation of size and dynamics of the inferior vena cava as an index of right-sided cardiac function. Am J Cardiol 1984;53:579-85.

[16] E. Ettinger IS. Angiocardiographic measurement of the cardiac segment of the inferior vena cava in health and in cardiovascular disease. Circulation 1962;26:508-15.
[17] P. Zielinski IM, E. Kowalik, A. Mierzynska, A. Klisiewicz, M. Kowalczyk, P. Kwiatek, M. Kusmierczyk, J. Rozanksi, M. Kowalski, P. Hoffman. Is there any role for computed tomography imaging in anticipating the functional status in adults late after total cavopulmonary connection? A retrospective evaluation. Kardiologia Polska 2019.
[18] Itatani K, Miyaji K, Tomoyasu T, Nakahata Y, Ohara K, Takamoto S et al. Optimal conduit size of the extracardiac Fontan operation based on energy loss and flow stagnation. Ann Thorac Surg 2009;88:565-72; discussion 72-3.
[19] Bossers SS, Cibis M, Gijsen FJ, Schokking M, Strengers JL, Verhaart RF et al. Computational fluid dynamics in Fontan patients to evaluate power loss during simulated exercise. Heart 2014;100:696-701.
[20] Restrepo M, Mirabella L, Tang E, Haggerty CM, Khiabani RH, Fynn-Thompson F et al. Fontan pathway growth: a quantitative evaluation of lateral tunnel and extracardiac cavopulmonary connections using serial cardiac magnetic resonance. Ann Thorac Surg 2014;97:916-22.
[21] Sundareswaran KS, Pekkan K, Dasi LP, Whitehead K, Sharma S, Kanter KR et al. The total cavopulmonary connection resistance: a significant impact on single ventricle hemodynamics at rest and exercise. Am J Physiol Heart Circ Physiol 2008;295:H2427-35.
[22] Whitehead KK, Pekkan K, Kitajima HD, Paridon SM, Yoganathan AP, Fogel MA. Nonlinear power loss during exercise in single-ventricle patients after the Fontan: insights from computational fluid dynamics. Circulation 2007;116:I165-71.
[23] Schmitt B, Steendijk P, Ovroutski S, Lunze K, Rahmanzadeh P, Maarouf N et al. Pulmonary vascular resistance, collateral flow, and ventricular function in patients with a Fontan circulation at rest and during dobutamine stress. Circ Cardiovasc Imaging 2010;3:623-31.
[24] Rijnberg FM, van Assen HC, Hazekamp MG, Roest AAW, Westenberg JJM. Hemodynamic Consequences of an Undersized Extracardiac Conduit in an Adult Fontan Patient Revealed by 4-Dimensional Flow Magnetic Resonance Imaging. Circ Cardiovasc Imaging 2021;14:e012612.
[25] Goldberg DJ, Avitabile CM, McBride MG, Paridon SM. Exercise capacity in the Fontan circulation. Cardiol Young 2013;23:824-30.
[26] Evans WN, Acherman RJ, Mayman GA, Galindo A, Rothman A, Winn BJ et al. The Rate of Hepatic Fibrosis Progression in Patients Post-Fontan. Pediatr Cardiol 2020;41:905-09.
[27] Schwarz EL, Kelly JM, Blum KM, Hor KN, Yates AR, Zbinden JC et al. Hemodynamic performance of tissue-engineered vascular grafts in Fontan patients. NPJ Regen Med 2021;6:38.
[28] Rijnberg FM, van Assen HC, Juffermans JF, Kroft LJM, van den Boogaard PJ, de Koning PJH et al. Reduced scan time and superior image quality with 3D flow MRI compared to 4D flow MRI for hemodynamic evaluation of the Fontan pathway. Sci Rep 2021;11:6507.
[29] van der Woude SFS, Rijnberg FM, Hazekamp MG, Jongbloed MRM, Kenjeres S, Lamb HJ et al. The Influence of Respiration on Blood Flow in the Fontan Circulation: Insights for Imaging-Based Clinical Evaluation of the Total Cavopulmonary Connection. Front Cardiovasc Med 2021;8:683849.
[30] Hsia TY, Khambadkone S, Deanfield JE, Taylor JF, Migliavacca F, De Leval MR. Subdiaphragmatic venous hemodynamics in the Fontan circulation. J Thorac Cardiovasc Surg 2001;121:436-47.

Supplementary materials

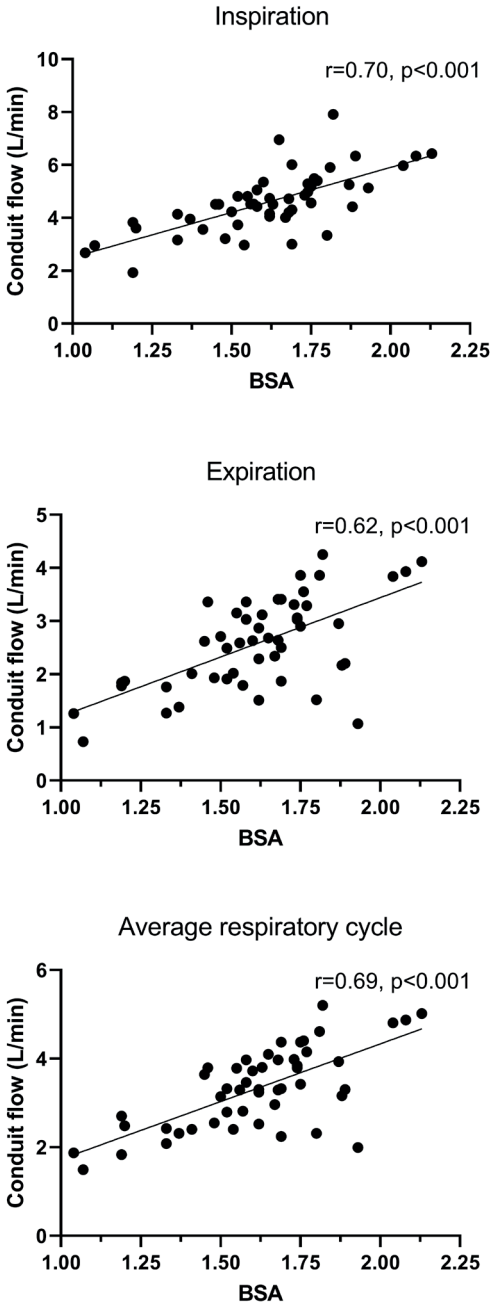

Supplemental Figure 1. A moderate to strong relationship is shown between BSA (Haycock) and conduit flow. However, important variability is observed in flow rates for patients with similar BSA

Supplemental material 1: 2D real-time flow MRI methodology

Multiple steps were performed to determine flow rates along the average respiratory cycle, inspiration and expiration from 2D real-time flow MRI acquisitions.

Philips physiology log files (PHYSLOG) were exported from the scanner for offline analysis of the respiratory signal at time of each 2D real-time flow acquisition. From these PHYSLOG files, the part of the respiratory signal corresponding to the 2D real-time flow acquisition was determined based on the manual start marker (marker value 100) and the stop marker (marker value 20) of each 2D flow acquisition (Supplemental Figure 1A-B).

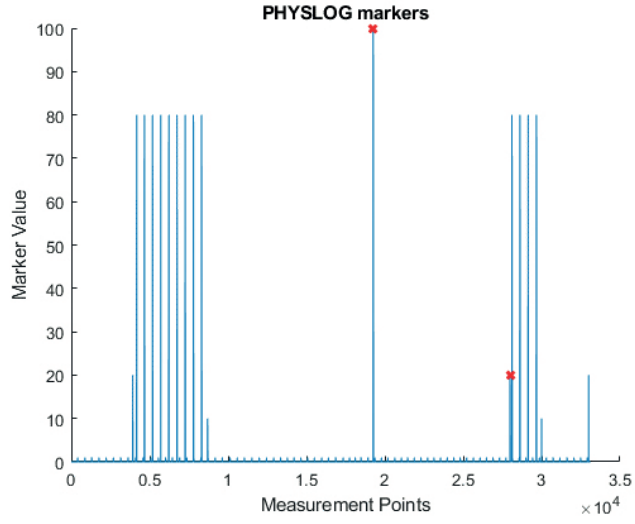

Supplemental Figure 1A

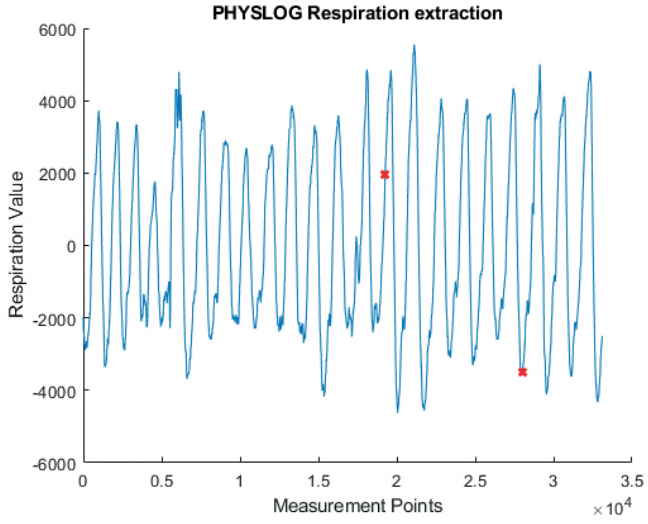

Supplemental Figure 1B

Since the start marker is known to not properly synchronize with the onset of the first flow volume[1], the duration of the respiratory signal from the PHYSLOG file slightly exceeded the duration of the corresponding flow acquisition. Therefore, the difference in duration between the respiratory signal and flow acquisition was removed from the first part of the respiratory signal (Supplemental Figure 1C, red part).

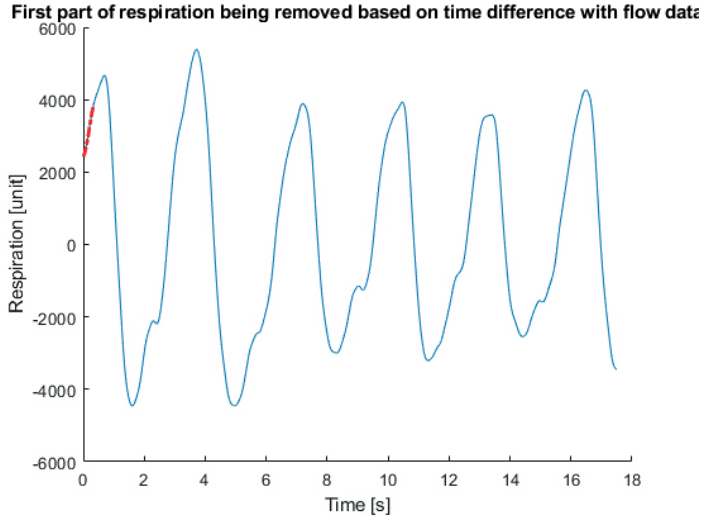

Supplemental Figure 1C

In general 2-4 consecutive respiratory cycles were extracted from the respiratory curve and subsequently divided into inspiration and expiration. Expiration was defined as the start of the downward deflection from the maximum value (Supplemental Figure 1D, blue). Inspiration started at the (last) bendpoint in the upward signal (Supplemental Figure 1D, green). The presence of an end-expiratory, upward drift of the respiratory signal towards the baseline was the reason why the start of the upward signal can not be used to mark the start of the inspiration.

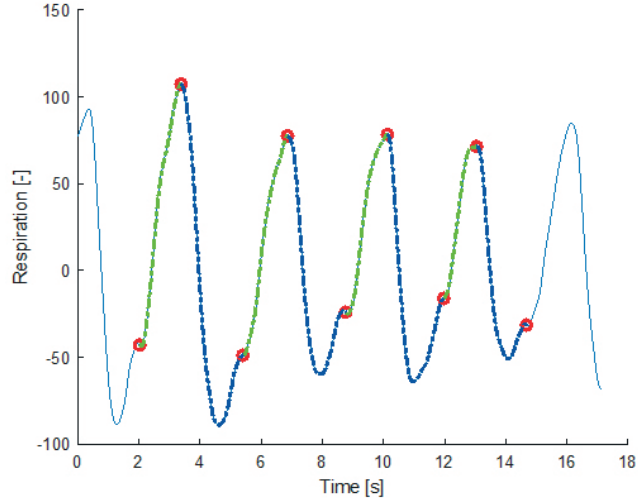

Supplemental Figure 1D

Subsequently, the flow and velocity curve were divided into the corresponding inspiratory and expiratory parts (Supplemental Figure 1E, showing the flow curve only).

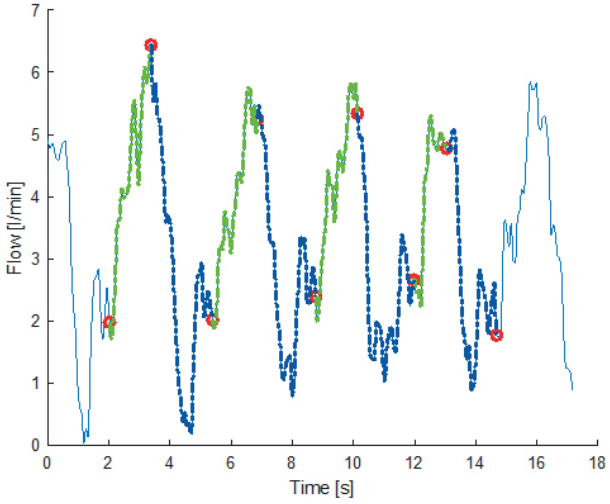

Supplemental Figure 1E

A single, average curve (Supplemental Figure 1H) was derived from the 2-4 individual inspiratory (Supplemental Figure 1F) and expiratory (Supplemental Figure 1G) curves using interpolation. Flow and velocity parameters were determined based on the average curves.

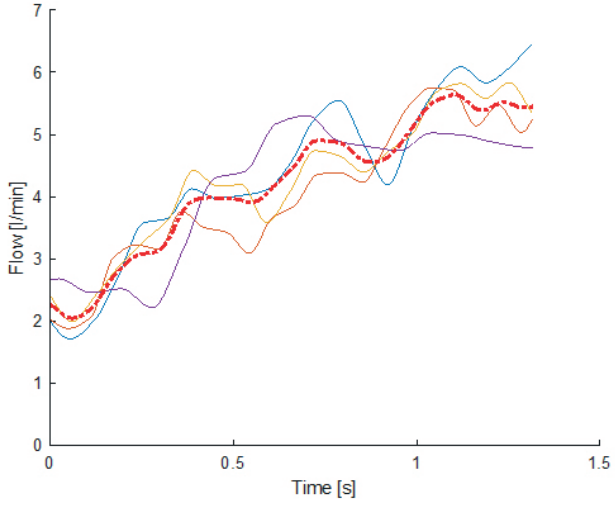

Supplemental Figure 1F

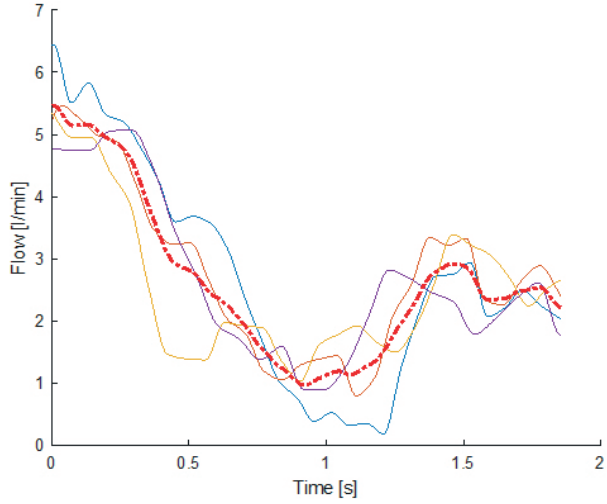

Supplemental Figure 1G

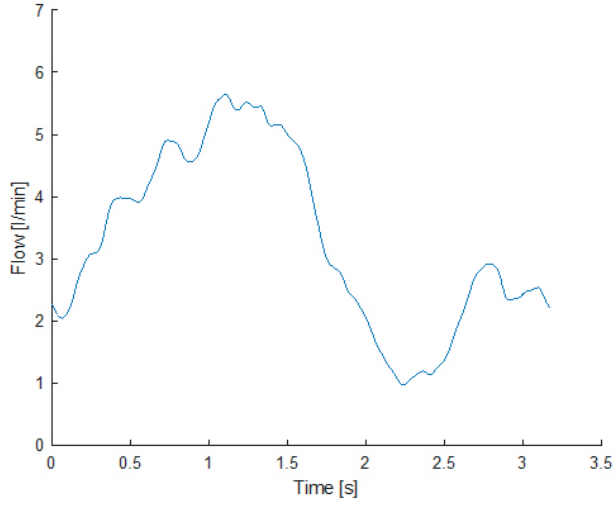

Supplemental Figure 1H

To acquire the real-time HV flow curve, the average inspiratory and expiratory flow curves from the IVC and conduit were aligned using interpolation. Subsequently, based on conservation of mass, HV flow was determined by subtracting IVC flow from conduit flow (Supplemental Figure 1i).

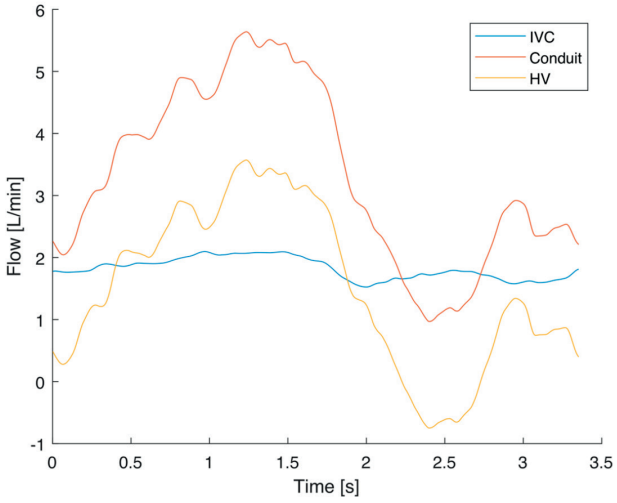

Supplemental Figure 1i

References

1. https://nl.mathworks.com/matlabcentral/fileexchange/42100-readphilipsscanphyslog-filename-channels-skipprep

Supplemental Table 1. 2D realtime flow MRI details

MRI details	2D realtime PC-MRI
Slice thickness (mm)	6
Acquired in-plane spatial resolution	2.5 x 2.5
Reconstructed in-plane spatial resolution (mm)	1.12 x 1.12
Temporal resolution	63-67ms
Nr of samples	250
ECG-gating	-
Respiratory compensation	-
Flip angle	20
TR (ms)	16
TE (ms)	8.7
Acceleration methods	SENSE factor 3, EPI 11

mm; millimetre, ECG; electrocardiogram, PC-MRI; phase contrast, MRI; magnetic resonance imaging